Effects of the Dynamical Scattering on the Molecular Images in High Resolution Electron Microscopy (Commemoration Issue Dedicated to Professor Keinosuke Kobayashi on the Occasion of His Retirement)

AUTHOR(S):

Ishizuka, Kazuo; Uyeda, Natsu

Bull. Inst. Chem. Res., Kyoto Univ., Vol. 55, No. 2, 1977

Effects of the Dynamical Scattering on the Molecular Images in High Resolution Electron Microscopy

Kazuo ISHIZUKA and Natsu UYEDA*

Received June 10, 1977

The wave functions and the scattering amplitudes of the crystal of chlorinated Cu-phthalocyanine were calculated based on the multi-slice formula of the dynamical scattering theory. A direct correlation between the intensity of the wave function and the specimen structure was obtained for the crystal of the thickness below 180 or 120 Å for 500 or 100 kV electrons respectively. Molecular images based on the dynamical scattering were synthesized by taking spherical aberration and defocusing effects into account. Although the condition for the kinematical approximation was not satisfied, the images similar to the kinematical ones were obtained at the Scherzer focus for the crystal of the thickness below 100 Å for both 500 kV electrons (C_s=1.0 mm) and 100 kV electrons (C_s=1.4 mm).

I. INTRODUCTION

In our previous papers,[1,2] high resolution molecular images of the thin crystal of chlorinated Cu-phthalocyanine were simulated within the kinematical approximation for a conventional 100 kV electron microscope and a special 500 kV microscope[3] installed in our institute. The image at best focusing condition resolved molecular details in the bright field mode for 500 kV electrons with the spherical aberration coefficient C_s of 1.0 or 1.8 mm. The simulated images for 100 kV electrons with C_s=1.4 mm only showed the molecular shape without the resolution of heavy atoms. The simulated images by the kinematical approximation showed qualitative agreements with the original electron micrographs,[1,4,5] although the specimens for these micrographs were exceedingly thick to hold this approximation. To estimate the maximum thickness of specimen which gives the kinematical like image, the molecular image should be calculated by considering the dynamical scattering effect.

Cowley and Moodie[6] have formulated the multi-slice method to calculate dynamical electron scattering, and a computing technique was summarized by Goodman and Moodie.[7] Extensive applications of this method to the electron microscope image simulation have been made by an Australian school.[8~10] The basis of the multi-slice formula was confirmed by its strict derivation from the Schrödinger equation, and a new computing technique of the multi-slice calculation was devised on the basis of Fourier transforms by the present authors.[11] This paper deals with the synthesized molecular image from the dynamical scattering and its comparison with that from the kinematical scattering. The critical specimen thickness which sets the upper limit for the specimen structure to be reflected by the synthesized molecular image is estimated for the model

* 石塚和夫, 植田 夏 : Laboratory of Crystal and Powder Chemistry, Institute for Chemical Research, Kyoto University Uji, Kyoto-Fu 611.

specimen of hexadecachloro Cu-phthalocyanine for 500 and 100 kV electrons.

II. METHOD

The effect of dynamical scattering of electrons on the high resolution electron micrographs is checked by simulating the molecular images of the crystal of chlorinated Cu-phthlocyanine in a monoclinic form with the crystal data:[1)]

$$a=19.62\ \text{Å},\quad b=26.04\ \text{Å},\quad c=3.76\ \text{Å},\quad \beta=116.5°.$$

Figure 1 shows a schematic representation of the model structure projected along c-axis, which has a plane symmetry cmm.

II.1 Scattering Calculations

The multi-slice formula gives the wave function at the n-th slice ψ_n in terms of that at (n-1)-th slice ψ_{n-1}:

$$\psi_n(xy)=[\psi_{n-1}(xy)\cdot q(xy)]*p(xy), \tag{1}$$

where $*$ denotes a convolution, and q and p represent a phase grating and a propagation functions respectively.[11)] The phase grating function is defined by the projected potential energy V_p within the slice as

$$q(xy)=\exp\left\{-\frac{i}{\hbar v}V_p(xy)\right\}, \tag{2}$$

and the propagation function is defined as

$$p(xy)=\frac{i}{\lambda}\frac{1}{\Delta z}\exp\left\{i\frac{2\pi}{\lambda}\frac{x^2+y^2}{2\Delta z}\right\}, \tag{3}$$

where v is the velocity of the incident electrons and Δz is the slice thickness.

The dynamical scattering amplitudes based on this multi-slice method are computed for 500 and 100 kV electrons with the programs developed previously.[11)] The incident direction of the electrons is assumed to coinside with the c-axis of the crystal. The slice thickness and the number of beams included in the multi-slice iteration are 2 unit cells and

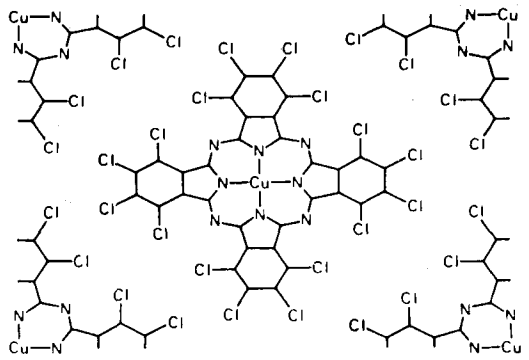

Fig. 1. A schematic representation of the model specimen structure which shows the c-axis projection of one unit cell. Non-carbon atoms are indicated.

about 4000 beams for 500 kV electrons, and one unit cell and about 2000 beams for 100 kV electrons.

II.2 Image Calculations

The molecular images are synthesized from the dynamical scattering amplitudes after the same method discussed in the previous papers.[1,2] The normal coherent illumination and the coincidence between the optic axis and c-axis of the crystal are assumed. The spherical aberration and the defocusing effects are taken into account in the image formation. The aberration function χ of the scattering angle α is defined as

$$\chi(\alpha)=\frac{2\pi}{\lambda}\left\{\left(\frac{\Delta f}{2}\right)\alpha^2-\left(\frac{C_s}{4}\right)\alpha^4\right\}, \tag{4}$$

where C_s is the spherical aberration coefficient of an objective lens, Δf the defocusing value (a positive value for underfocusing). A scattering vector h is related with α as $h=\alpha/\lambda$. A circular aperture and an annular aperture both positioned symmetrically to the optic axis are assumed for the bright field mode and the dark field mode respectively. Here the bright field mode or the dark field mode denotes that the transmitted beams satisfy the condition that $h\leq h_{\max}$ or $h_{\min}\leq h\leq h_{\max}$ respectively.

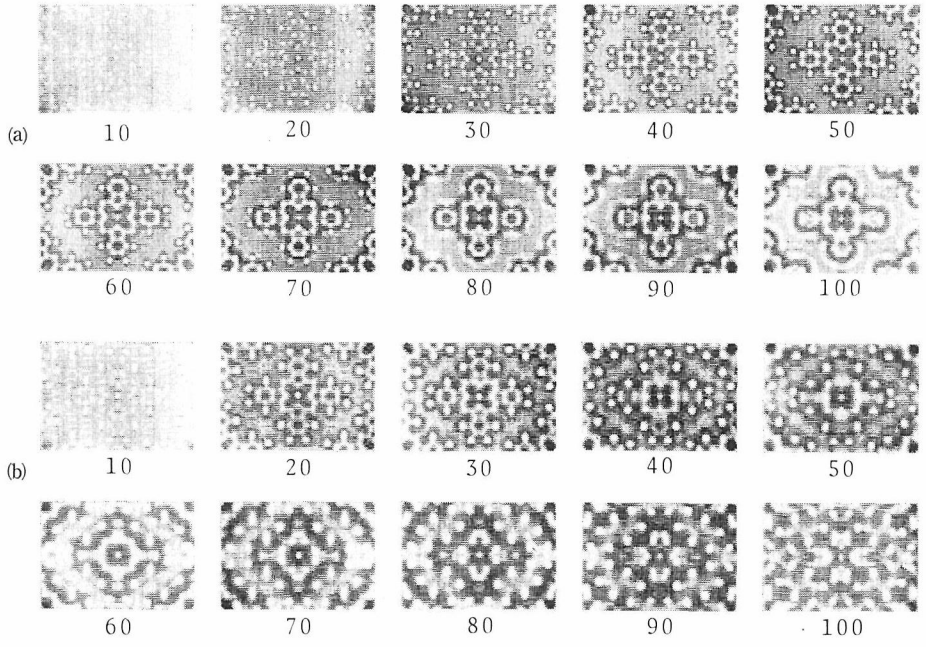

Fig. 2. Probability distribution of the transmitted electrons at the various crystal thicknesses (the number of unit cells along c-axis): (a) for 500 kV and (b) for 100 kV electrons. Light regions represent high electron density. Simple relation between the model structure and the probability distribution are observed for the crystal of the thickness below 50 or 30 cells for 500 or 100 kV electrons respectively.

III. RESULTS

III.1 Wave Functions

The wave function at the under surface of the specimen should represent the correct specimen structure in a simple fashion in order that the simulated image reveals the molecular details. Some results of the intensity distributions of the wave functions obtained at several specimen thicknesses are shown in Fig. 2, where lighter colored regions represent a higher electron density. Since the model specimen was assumed to be a pure phase object, the electron density difference for thin crystal was relatively small. When the crystal thickness was increased, the electrons converged into each atom position and low electron density areas appeared in its surrounding regions. The probability density at the centers of copper, chlorine and nitrogen atoms are shown more quantitatively as a function of the specimen thickness in Fig. 3. The densities increase monotonically up to the specimen thicknesses of 40 and 25 cells for 500 and 100 kV electrons respectively. A resolution deterioration due to the electron divergence by the multiple scattering is also appreciated on the probability distribution maps in Fig. 2. A resolution deterioration starts at thinner specimen thickness for 100 kV electrons than for 500 kV electrons, since the scattering angle is larger in the former case than in the latter one. It may be concluded that the simple relation between the wave function and the specimen structure is held when the specimen thickness does not exceed 50 or 30 cells for 500 or 100 kV electrons respectively.

III.2 Molecular Images

For 500 kV electrons with C_s=1.0 mm and h_{max}=0.620 Å^{-1}, the bright field images were synthesized with a series of defocusing value (through-focusing) by using the dy-

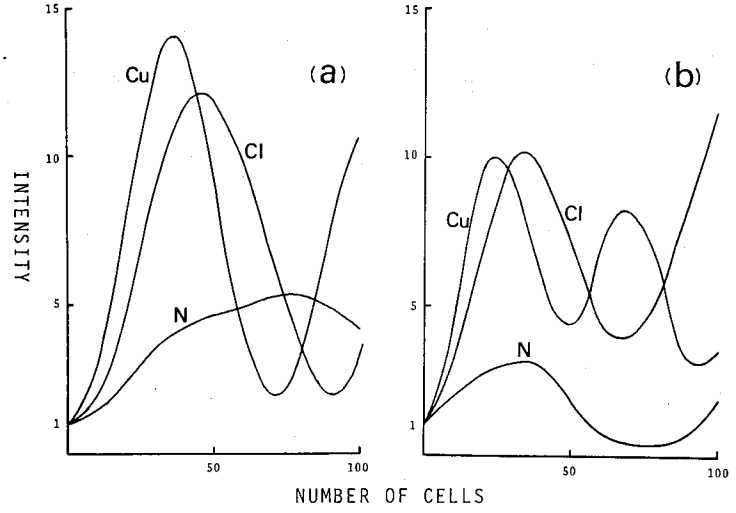

Fig. 3. Electron densities at the centers of copper, chlorine and nitrogen atoms as a function of the specimen thickness: (a) for 500 kV and (b) for 100 kV electrons. It shows the convergence of electrons at the atom sites up to the specimen thickness of 40 or 25 cells for 500 or 100 kV electrons respectively.

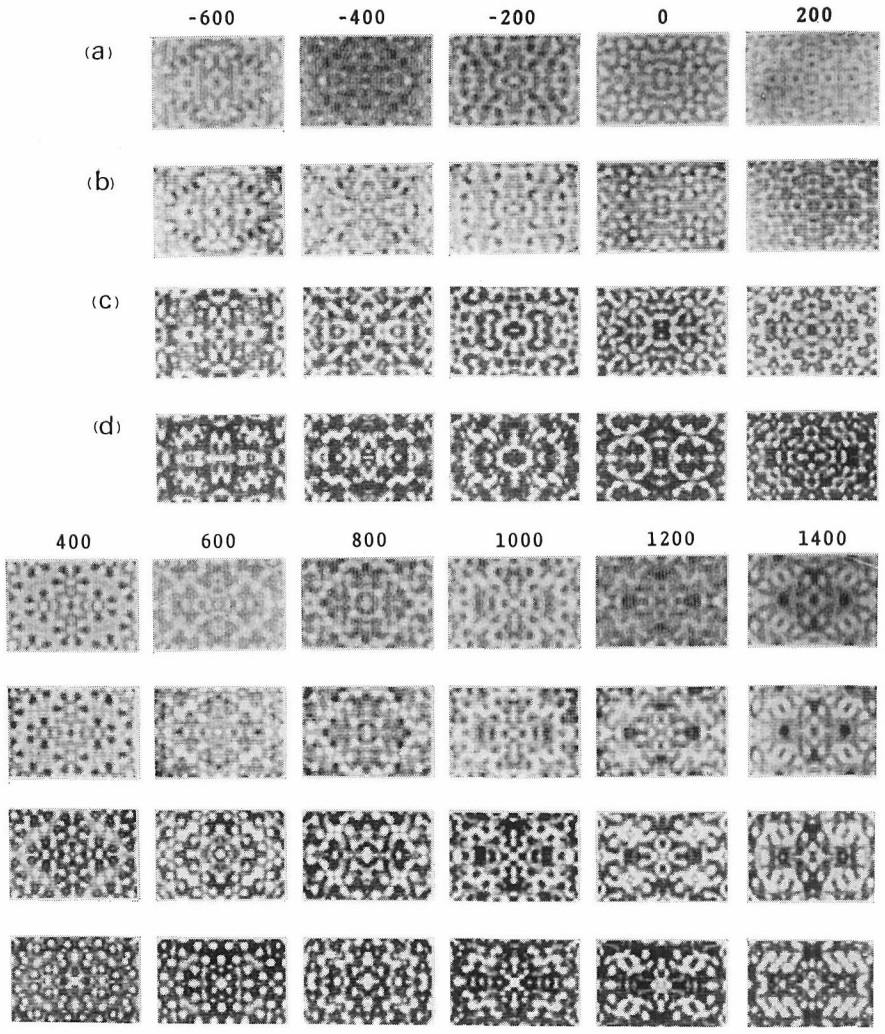

Fig. 4. Some results of through-focusing calculation of the dynamical bright field images of specimen thicknesses of 10 (b), 30 (c), and 50 (d) cells and the kinematical ones (a) for 500 kV electrons with C_s=1.0 mm (h_{max}=0.620 Å^{-1}). The images of 10 and 30 cells thicknesses are very similar to the kinematical ones.

namical scattering amplitudes at several specimen thicknesses. Some through-focusing bright field images of the specimen thicknesses of 10, 30, and 50 cells and the reproduced kinematical images are shown in Fig. 4. The through-focusing images of 10 and 30 cells thicknesses were very similar to the kinematical ones and the best image was obtained at the Scherzer focus Δf=400 Å[1] (the optimum focus position in the kinematical approximation.)[12] The image contrast of the heavy atoms began to decrease in the best image of 30 cells and reversed in the image of 50 cells. A series of the molecular images of various crystal thicknesses at the Scherzer focus is shown in Fig. 5. The contrast of the heavy atoms at 100 cells thickness become again dark similar to the kinematical contrast,

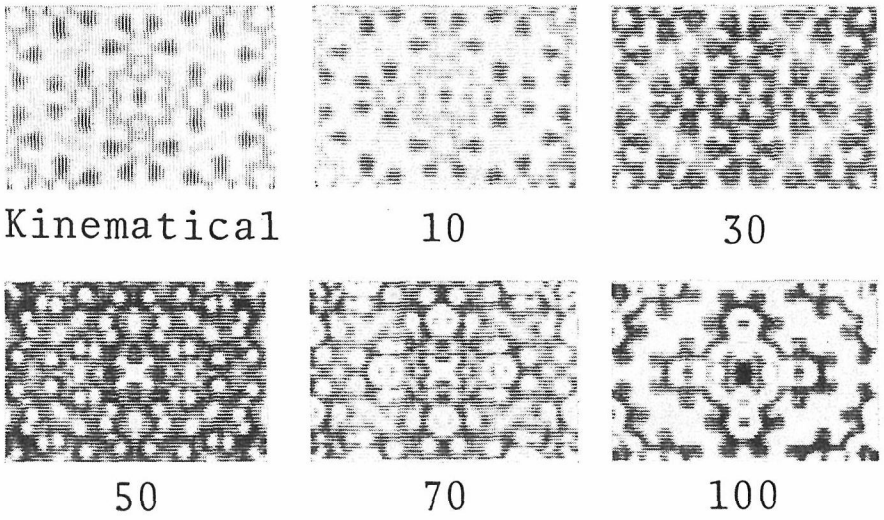

Fig. 5. Images of specimens of several thicknesses at the Scherzer focus (400 Å under-focus) for 500 kV electrons. The kinematical like images are obtained for the specimen of the thickness below 20～30 cells.

but the image details are lost appreciably by the dynamical multiple scattering effect. It is concluded that the image similar to the kinematical one will be obtained when the specimen thickness does not exceed 20～30 cells. Here the best image will be obtained at the Scherzer focus.

Another series of images was synthesized for 500 kV electrons with C_s=1.8 mm and h_{max}=0.528 Å^{-1}. These images showed the same dynamical effects as in the case of C_s= 1.0 mm, *i.e.,* (a) the images were similar to the kinematical ones when the crystal thickness does not exceed 20～30 cells, and (b) the best image was obtained at the Scherzer focus (Δf=550 Å).[1)]

The through-focusing bright field images were synthesized by using the dynamical scattering amplitudes to estimate the performance of the present-day conventional electron microscope operated at 100 kV accelerating voltage with C_s=1.4 mm and h_{max}=0.292 Å^{-1}. Some results of the dynamical images of the specimen thicknesses of 10, 20, and 30 cells and the kinematical images are shown in Fig. 6. The through-focusing images of 10 and 20 cells thicknesses resembled closely to the kinematical ones, and the best image reflecting the molecular shape of a four-leaf clover was obtained at Δf=800 Å[1)] (the Scherzer focus) for each crystal thickness. The images of various crystal thicknesses at the Scherzer focus are shown in Fig. 7. For 100 kV electrons with C_s=1.4 mm, the image like a four-leaf clover will be obtained for the specimen of the thickness below 20～ 30 cells.

Dark field images were synthesized by using the dynamical scattering amplitudes for 500 kV electrons (C_s=1.0 mm, h_{min}=0.02 Å^{-1} and h_{max}=0.620 Å^{-1}) and for 100 kV electrons (C_s=1.4 mm, h_{min}=0.02 Å^{-1} and h_{max}=0.292 Å^{-1}) as in the case of the kinematical calculation.[2)] They showed the same inferiority to the bright field images as in the kinematical case, *i.e.,* (a) the molecular details were hardly recognized even in the best focus image, and (b) some ghost peaks appeared in all the images.

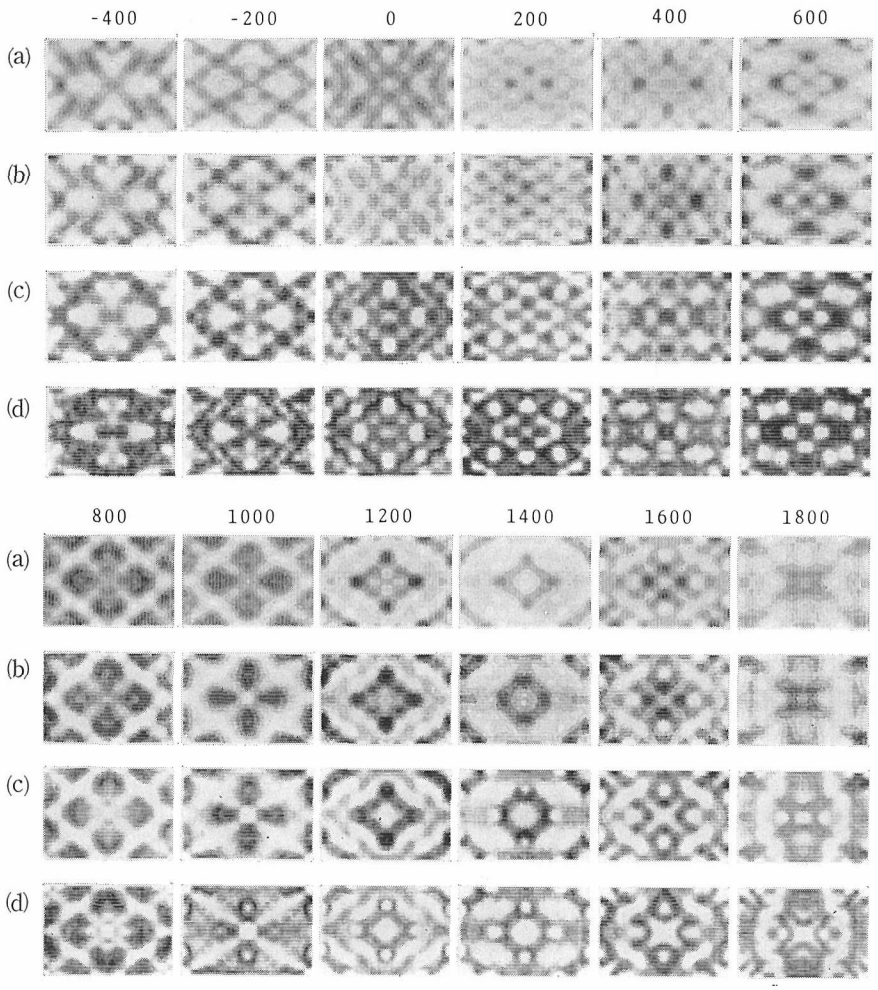

Fig. 6. Some results of the through-focusing bright field images synthesized with the dynamical scattering amplitudes at the specimen thicknesses of 10 (b), 20 (c) and 30 (d) cells and with the kinematical scattering amplitudes (a) for 100 kV electrons with C_s=1.4 mm (h_{max}=0.292 Å^{-1}). The images of 10 and 20 cells hicknesses are very similar to the kinematical ones.

IV. CONCLUSION

The dynamical scattering effects destroy a simple relationship between the wave function and the specimen structure when the crystal thickness exceeds its critical value: 50 cells for 500 kV or 30 cells for 100 kV electrons in the case of chlorinated Cu-phthalocyanine. The difference of these critical thicknesses can be directly deduced from the factor $\hbar v$ in the phase grating equation (2), since $\hbar v$ equals to 1703 or 1082 eV·Å for 500 or 100 kV electrons respectively. The images similar to the kinematical ones are obtained even from the specimen which does not satisfy the condition for the kinematical approximation: $V_p(xy)/\hbar v \ll 1$. At the center of the copper atom, this condition is satisfied only for the specimen of the thickness below 3 or 2 cells for 500 kV or 100 kV

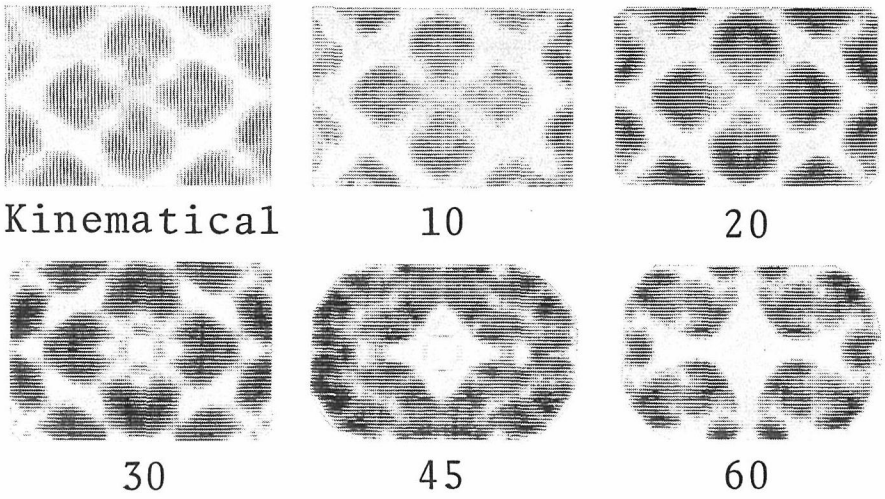

Fig. 7. Images of specimens of several thicknesses at the Scherzer focus (800 Å under-focus) for 100 kV electrons. The kinematical like images are obtained for the specimen of the thickness below 20～30 cells.

electrons respectively. The deviation from the kinematical image due to the dynamical scattering and the microscope aberration starts at the crystal thickness of 20～30 cells for both 500 kV electrons with C_s=1.0 mm and 100 kV electrons with C_s=1.4 mm. The electron optical aberration limits the specimen thickness giving the kinematical like image in the case of 500 kV electrons. The best image is obtained at the Scherzer focus even for the crystal where the dynamical effect is appreciable. The bright field images with the dynamical scattering amplitudes are superior to the dark field ones for high resolution molecular structure investigation as concluded in the kinematical calculations.[2)]

The effects of the beam divergence[10)] and the chromatic aberration[13)] should be included in the simulation and the image processing of the crude micrographs should be necessary in oder to compare the experimental images quantitatively with the simulated ones.

ACKNOWLEDGMENT

This paper is dedicated to Emeritus Professor K. Kobayashi on the commemoration of his retirement, to whom the authors wish to thank for his introduction to the high resolution work and his continuous encouragement. KI thanks the Matsunaga Science Foundation for a financial support during preliminary work of this report.

REFERENCES

(1) N. Uyeda and K. Ishizuka, *J. Electron Microsc.*, **23**, 79 (1974).
(2) K. Ishizuka and N. Uyeda, *Buil. Inst. Chem. Res., Kyoto Univ.*, **53**, 200 (1975).
(3) K. Kobayashi, E. Suito, N. Uyeda, M. Watanabe, T. Yanaka, T. Etoh, H. Watanabe, and M. Moriguchi, *Proc. Eighth Intern'l Congr. Electron Microsc., Canberra,* **1**, 30 (1974).

(4) N. Uyeda, K. Ishizuka, Y. Saito, Y. Murata, K. Kobayashi, and M. Ohara, *ibid.*, **1**, 266 (1974).
(5) N. Uyeda, T. Kobayashi, K. Ishizuka, Y. Fujiyoshi, and K. Kobayashi, *Sixth Europ. Congr. Electron Microsc., Jerusalem*, **1**, 79 (1976).
(6) J. M. Cowley and A. F. Moodie, *Acta Cryst.*, **10**, 609 (1957).
(7) P. Goodman and A. F. Moodie, *Acta Cryst.*, **A30**, 280 (1974).
(8) D. F. Lynch and M. A. O'Keefe, *Acta Cryst.*, **A28**, 536 (1972).
(9) M. A. O'Keefe, *Acta Cryst.*, **A29**, 389 (1973).
(10) M. A. O'Keefe and J. V. Sanders, *Acta Cryst.*, **A31**, 307 (1975).
(11) K. Ishizuka and N. Uyeda, *Acta Cryst*, **A31** (in the press).
(12) O. Scherzer, *J. Appl. Phys.*, **20**, 20 (1949).
(13) P. L. Fejes, *Acta Cryst.*, **A33**, 109 (1977).